An evaluation of ISFET sensors for coastal pH monitoring applications

Karen McLaughlin [a,*], Andrew Dickson [b], Stephen B. Weisberg [a], Kenneth Coale [c],
Virginia Elrod [d], Craig Hunter [c], Kenneth S. Johnson [d], Susan Kram [b,1], Raphael Kudela [e],
Todd Martz [b], Kendra Negrey [e], Uta Passow [f], Frank Shaughnessy [g], Jennifer E. Smith [b],
Dawit Tadesse [h], Libe Washburn [f], Kyle R. Weis [g]

[a] Southern California Coastal Water Research Project Authority, Costa Mesa, CA 92626, United States
[b] Scripps Institution of Oceanography, University of California San Diego, La Jolla, CA, 92093, United States
[c] Moss Landing Marine Laboratories, 8272 Moss Landing Road, Moss Landing, CA 95039, United States
[d] Monterey Bay Aquarium Research Institute, Moss Landing, CA, 95039, United States
[e] University of California, Santa Cruz, CA 95064, United States
[f] Marine Science Institute, University of California Santa Barbara, CA 93106, United States
[g] Humboldt State University, Arcata, CA 95521, United States
[h] California State Water Resources Control Board, Sacramento, CA 95814, United States

ARTICLE INFO

ABSTRACT

The accuracy and precision of ion sensitive field effect transistor (ISFET) pH sensors have been well documented, but primarily by ocean chemistry specialists employing the technology at single locations. Here we examine their performance in a network context through comparison to discrete measurements of pH, using different configurations of the Honeywell DuraFET pH sensor deployed in six coastal settings by operators with a range of experience. Experience of the operator had the largest effect on performance. The average difference between discrete and ISFET pH was 0.005 pH units, but ranged from −0.030 to 0.083 among operators, with more experienced operators within ±0.02 pH units of the discrete measurement. In addition, experienced operators achieved a narrower range of variance in difference between discrete bottle measurements and ISFET sensor readings compared to novice operators and novice operators had a higher proportion of data failing quality control screening. There were no statistically significant differences in data uncertainty associated with sensor manufacturer or deployment environment (pier-mounted, flowthrough system, and buoy-mounted). The variation we observed among operators highlights the necessity of best practices and training when instruments are to be used in a network where comparison across data streams is desired. However, while opportunities remain for improving the performance of the ISFET sensors when deployed by less experienced operators, the uncertainty associated with their deployment and validation was several-fold less than the observed natural temporal variability in pH, demonstrating the utility of these sensors in tracking local changes in acidification.

1. Introduction

Seawater pH is often used as a key parameter for understanding the impacts of ocean acidification (OA) on coastal ecosystems. These ecosystems are vulnerable to ecological and biogeochemical perturbations from OA (Doney et al., 2009; Howarth et al., 2011), which are affected by factors such as freshwater inputs, tidal forcing, water stratification, nutrient over-enrichment, algal blooms, and hypoxia (Fabry et al., 2008; Borges and Gypens, 2010). These perturbations may also take place within a background of acidification associated with the upwelling of low pH waters, such as on the US West Coast. Thus, there is a trend towards increased monitoring of pH in coastal environments to both understand the inherent variability of coastal pH and aid in development of a mechanistic understanding of the roles of coastal feedbacks and interactions (Hofmann et al., 2011; Boehm et al., 2015).

Ion sensitive field effect transistor (ISFET) pH sensors have been shown to be stable and accurate for monitoring fine-scale changes in pH in seawater (Martz et al., 2010) and have rapidly become a preferred method for high frequency measurements of pH in ocean and nearshore monitoring (Hofmann et al., 2011; Kroeker et al., 2011; Yu et al., 2011; Johnson et al., 2016). They are also easy to deploy, requiring minimal maintenance during monthly or longer deployments, and deployable in a variety of habitat types (Hofmann et al., 2011). However, quantification of the accuracy and precision of ISFET sensors has primarily been conducted using individual instruments deployed by ocean chemistry specialists with a high degree of experience. While such studies provide understanding of temporal patterns at a particular site, ISFET instruments are increasingly being incorporated into monitoring networks for regional studies of spatial and temporal patterns [e.g., the California Current Acidification Network McLaughlin et al., 2015, the Global Ocean Acidification Observing Network Newton et al., 2014]. Networked spatial comparisons can be confounded by the additional variability associated with use of sensors from different manufacturers, deployment in different habitat types, and the different levels of experience of the operator. Here we examine performance of ISFET sensors in a network context by comparing discrete measurements of pH to sensors deployed in a variety of environments at six coastal California sites by operators with a range of experience to gain insight into what additional uncertainty may be added across sites.

2. Materials and methods

ISFET sensors were evaluated in two ways. First, we quantified the number of short-term errant spikes and extent of instrument drift at each site. Second, we compared instrument readings to discrete bottle samples, collected at the same time and in close proximity to the sensors, that were processed for pH using both a spectrophotometric indicator dye technique and calculated from simultaneous measurement of dissolved inorganic carbon (DIC) and total alkalinity (TA). Uncertainty in ISFET sensor measurements was then compared to the observed variability at the sites as indicated by the natural range of pH values observed during each deployment. Natural variability in pH at each site was defined as the range of pH encompassing 90% of all observed pH values.

2.1. Sensors

ISFET sensors were deployed at six nearshore locations along the California coast with a range of pH variability (Fig. 1, Table 1); three were on stationary pier pilings (sites A, E, F), one on a moored buoy (C), and two in a flowthrough stream from a pumped water source (B, D). Stationary pier piling sensors were mounted at depths of 1–4 m (below the lowest, low tide line). The intake of the sensor at the moored, buoy sensor was at 20 cm depth (site C). Source water for the flowthrough system at site B was at the surface, and for site D was at 17 m. Four of the sites were in coastal ocean waters (B, D, E, F), one in an enclosed bay (A) and one at the mouth of a small slough (C).

Independent operator groups deployed sensors, and collected and preserved discrete samples at each site. Of these groups, three were using the sensors for the first time (A, B, D) and are hereafter referred to as "novices". The remaining three had varying levels of prior experience with the instruments (C, E, F) and are hereafter referred to as "experienced".

Three configurations of the Honeywell DuraFET ISFET pH transducer were used among sites: (1) a commercially available system from Honeywell consisting of a DuraFET sensor (with internal chloride ion reference electrode) coupled to a controller box (Honeywell UDA2182), (2) a commercially available system from Satlantic

Fig. 1. Location of ISFET deployments along California coastline.

("SeaFET") consisting of a DuraFET and an external chloride ion selective reference electrode (wherein the external reference electrode was preferred except when salinity dropped below 20, due to unquantifiable uncertainties in the liquid junction potential), and (3) prototype versions of configuration (2) that were constructed in the Martz Lab at the Scripps Institution of Oceanography (SIO) and at the Monterey Bay Aquarium Research Institute (MBARI) (Martz et al., 2010). Sensors collected instantaneous pH measurements at variable frequencies depending on the site. All configurations of the ISFET included a thermistor. A subset of sites had co-located sensor packages collecting a variety of ancillary data including temperature, salinity, water depth (pressure), chlorophyll fluorescence, and dissolved oxygen (YSI 6600 data sonde, Sea Bird Electronics SBE37 Microcat, Sea Point chlorophyll fluorometer). Methods of instrument calibration, maintenance and biofouling minimization are described in Table 1.

2.2. Assessment of sensor operation

Analysis of the rate of change in pH with time was conducted to inspect the data for three conditions: (a) short-term, errant values that appear as unexplained spikes in the data record, (b) sensor instability at the start of deployment (sensor conditioning—see below), and (c) sensor failure that manifested as drift. Potentially errant pH measurements were flagged if the $\Delta pH/\Delta t ([pH_i - pH_j]/[t_i - t_j])$ over an interval of time exceeded ± 2 standard deviations from the deployment mean $\Delta pH/\Delta t$. If the flagged interval occurred as an isolated, anomalous spike, the record was classified as errant. If pH values around the flagged interval occurred in a series of similarly high or low pH values (e.g., an event of high or low pH), the record was maintained.

Sensor instability at the start of the deployment, likely due to reconditioning of the sensor in a new environment (Bresnahan et al., 2014), was indicated as the time period with highly variable $\Delta pH/\Delta t$ relative to the mean $\Delta pH/\Delta t$ at the beginning of the deployment and not otherwise associated with similar variability in temperature or salinity values over the same interval. Similarly, sensor drift due to biofouling or sensor failure (such as battery failure) was manifest as a segment of the time-series where measurements gradually decrease to improbable pH values (< 7.0 at salinities exceeding 30) or temperature measurements (< 0 °C). Values from sensors drifting due to sensor conditioning or other problems were deleted from the final dataset used to assess sensor

Table 1
Sampling locations and sensor information.

Site location	Sensor	Sample frequency (min)	Calibration	Biofouling counter-measures	Maintenance	Discrete sample collection
Pier-mounted site A Humboldt Bay, Chevron Dock (40.7776 and −124.1965) novice	Honeywell DuraFET III	5	Two point calibrations performed in 7.0 and 10.0 pH buffer solutions	Biofouling removed every 21–28 days during calibration	Sensor cleaned and maintained according to manufacturer specifications once every 21–28 days.	Discrete sample collected at sensor deployment depth with Wildco 2.2 L Alpha Horizontal Sampler and subsampled in to the Pyrex bottle through a Tygon tube
Flowthrough site B Santa Cruz Wharf (36.9603 and −122.0203) novice	Satlantic Ocean pH sensor	5	Calibrated to regression line developed with pH standards 7 and 10	Copper guard provided by Satlantic with the SeaFET sensor	Sensor fouling removed weekly	Discrete sample draw from flowthrough system conducted 5 cm downstream of sensor
Buoy site C Elkhorn Slough (36.8078 and −121.7710) experienced	Prototype SeaFET Ocean pH sensor	60	Calibrated in TRIS; TRIS pH validated with m-cresol purple dye method	Water was pumped through copper/nickel tubing from the intake to the pH flow cell	Sensor rinsed with ambient water every two months; Occasionally rinsed with freshwater or dilute hydrochloric acid and wiped with a cotton tipped applicator as necessary.	Discrete samples collected in proximity to buoy in 2.5 L Niskin bottle and subsampled in to the Pyrex bottle through a Tygon tube
Flowthrough site D Moss Landing Marine Labs (36.8025 and −121.7915) experienced	Honeywell DuraFET III	15	Calibrated to regression line developed with pH standards 6 and 10 as well as Tris and AMP buffers	Water was pumped through copper/nickel tubing	Sensor cleaned and maintained according to manufacturer specifications once or twice monthly depending on sediment load	Discrete sample draw from flowthrough system conducted 5 cm downstream of sensor
Pier-mounted site E Santa Barbara, Sterns Wharf (34.4092 and −119.6847) novice	Satlantic Ocean pH sensor	15	Calibrated in situ from parallel measurements	Flow through copper caps were installed over the SeaFET electrodes. Pressure cases were wrapped in tape to remove bio-fouling after recovery	Sensor cleaned and maintained according to manufacturer specifications every three months	Discrete samples collected in proximity to sensor deployment (horizontal and depth proximity) in 2 L Niskin bottle and subsampled in to the Pyrex bottle through a Tygon tube
Pier-mounted site F Scripps Pier (32.8669 and −117.2574) experienced	Prototype SeaFET Ocean pH sensor	15	Calibrated in TRIS; TRIS pH validated with m-cresol purple dye method	Copper mesh guard placed around the SeaFET sensor to prevent biofouling	Sensor cleaned and maintained according to manufacturer specifications every two months	Discrete samples collected in proximity to sensor deployment (horizontal and depth proximity) in 2 L Niskin bottle and subsampled in to the Pyrex bottle through a Tygon tube

performance (sensor measurements compared to bottle samples). Deleted segments for conditioning and drift included the series of values from the improbable value back to the portion of the dataset where the $\Delta\mathrm{pH}/\Delta t$ value was consistently within two standard deviations of the mean $\Delta\mathrm{pH}/\Delta t$.

2.3. Discrete sample analysis

Discrete samples were collected in close proximity (temporal and spatial) to sensor measurements in 500 mL Pyrex bottles. A single sample was collected for analysis of pH and total alkalinity (TA), and a separate sample was collected for dissolved inorganic carbon (DIC). For pier and buoy sites, separate samples for pH/TA and DIC were collected from Niskin bottles, and for flowthrough sites water was pumped into consecutive bottles. All bottles were overfilled by a minimum of 250 mL leaving ∼1% headspace and preserved with ∼120 µL of saturated mercury(II) chloride solution. Samples were sealed with a greased glass stopper secured with a rubber band and clip and stored at room temperature until analysis (Dickson et al., 2007). Field duplicates were conducted on 10%

of the samples. Discrete samples were shipped to and analyzed by Dr. Andrew Dickson's Laboratory at the Scripps Institution of Oceanography, University of California, San Diego.

Discrete pH was quantified in two ways: spectrophotometrically using an indicator dye technique, and calculated from measurements of DIC and TA. The spectrophotometric pH technique was based on the method described by Carter et al. (2013), estimating pH at 25 °C on the total hydrogen ion scale using purified m-cresol purple indicator dye and calibration equations developed by Liu et al. (2011). DIC was assayed by a gas extraction/coulometric procedure (Dickson et al., 2007) calibrated against seawater-based reference materials for which DIC had been certified by a vacuum extraction/manometric procedure (Dickson, 2001). TA was determined by a two-stage, potentiometric, open-cell titration using coulometrically analyzed hydrochloric acid (Dickson et al., 2003). CO_2 reference materials (produced by the Dickson Laboratory) were run as quality control for TA, DIC, and pH. The pH was calculated from samples of DIC and TA using CO2calc version 1.2.8 and is reported on the total hydrogen ion concentration scale at *in situ* temperature (Robbins et al., 2010). The CO2calc program (and

Table 2
Data quality screening results for each site.

Station	Dataset % complete after QA	% Eliminated at start of deployment (Conditioning issue)	% Eliminated due to drift to improbable values	% Eliminated due to Rogue data points
Pier-mounted site A	34%	40%	26%	0.1%
Flowthrough site B	96%	0%	4%	0.1%
Buoy site C	99%	0%	1%	0.05%
Flowthrough site D	96%	0%	4%	0.05%
Pier-mounted site E	71%	0%	29%	0.01%
Pier-mounted site F	>99%	0%	0%	0.05%
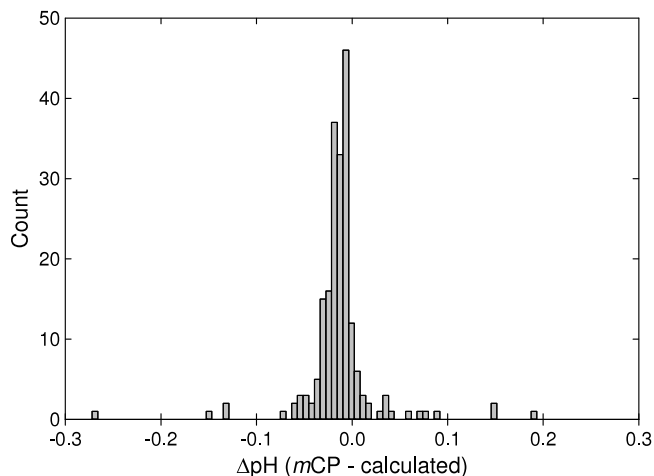
Fig. 2. Comparison of discrete, bottle pH measurements made using the m-cresol purple indicator dye method and discrete, bottle pH values calculated from measurements of dissolved inorganic carbon and total alkalinity for all sites.

the measured data for TA) was also used to convert discrete, spectrophotometric pH measurements to *in situ* temperatures. Program preferences were set to use carbonate system acid dissociation constants from Lueker et al. (2000), KHSO$_4$ dissociation constants from Dickson et al. (1990), and total boron from Lee et al. (2010).

Differences between the paired discrete, bottle measurements of pH and ISFET sensor measurements were not normally distributed. Therefore, comparisons between sites with different operator experience level, ISFET sensor configuration, and deployment type were evaluated using non-parametric Mann–Whitney Rank Sum Tests (SigmaPlot 12.5).

3. Results

3.1. Assessment of sensor operation

Errant data points and short periods of malfunction were present at all sites, but there were four sites (Sites B, C, D, and F) for which greater than 95% of data met the quality control assessment (Table 2, Supplemental Figures 1 and 2, Appendix A). For these sites, most of the unusable data occurred towards the end of the deployment periods and may be attributable to biofouling. Two sites had extended periods of unusable data (A, E). The dataset for Site E was generated by three different Satlantic sensors deployed in sequence, with most of the unusable data attributable to a single one of these sensors deployed between Dec 2012 and Mar 2013. This sensor functioned properly for about a month before exhibiting a sharp drift to improbable pH values that appeared unrelated to biofouling and were likely the result of instrument failure. The other two Satlantic sensors at Site E appeared to function appropriately throughout their respective deployments (Sep–Dec 2012 and Apr–Jun 2013, respectively). Site A was the only site to exhibit extreme variability in pH at the beginning of the time-series,

Table 3
Sensor pH range and performance relative to discrete measures of pH.

Comparison	n	Mean $\triangle \pm 2\sigma$
Comparison of field replicates		
mCP rep−mCP rep (Dickson Lab)	23	0.0114 ± 0.058
Calculated rep−calculated rep	24	0.0074 ± 0.015
Comparison of discrete pH measures		
mCP−calculated ($\triangle$pH$^{mCP\text{-}Calc}$)	203	-0.0154 ± 0.1038
Comparison of Discrete pH to Sensor pH		
Dickson mCP−ISFET ($\triangle$pH$^{mCP\text{-}FET}$)	163	0.005 ± 0.155
Calculated−ISFET ($\triangle$pH$^{Calc\text{-}FET}$)	166	0.021 ± 0.147

likely due to conditioning to the deployment environment, it also exhibited drifts towards improbable pH values at least twice during the remainder of its deployment, yet was seemingly functional between these events.

3.2. Agreement between discrete pH measurement methods

The mean difference between the two independent discrete measures of pH (spectrophotometric and calculated from DIC and TA, $\triangle$pH$^{mCP\text{-}Calc}$, $n = 203$) was -0.0154 with a spread ($\pm 2\sigma$ standard deviation) of ± 0.1038 pH units (Table 3, Fig. 2), comparable to what has been found by others in coastal settings (Hoppe et al., 2012; Wootton and Pfister, 2012). Agreement between field duplicates for pH calculated from DIC and TA (0.0074, $\pm 2\sigma = \pm 0.015$ pH units) was better than for field duplicates of pH estimated spectrophotometrically (0.0114, $\pm 2\sigma = \pm 0.058$ pH units).

3.3. Agreement between sensors and discrete pH measurements

The mean difference between the spectrophotometric pH value (mCP) and the ISFET sensor pH ($\triangle$pH$^{mCP\text{-}FET}$) for all sites was 0.005 with a $\pm 2\sigma$ standard deviation spread of ± 0.155 pH units (Table 3). However, agreement between measures at a single site was variable. The sites with the best agreement (sites C and F) had mean differences $\pm 2\sigma$ less than 0.02 ± 0.1 pH units, while the site with the worst agreement (A) was over double that amount (mean difference $\pm 2\sigma = 0.05 \pm 0.23$ pH units) (Table 4, Fig. 3). Most of the sites did not have a meaningful bias in the $\triangle p^{mCP\text{-}FET}$, with mean differences within ± 0.03 pH units of 0; however, two sites (Sites A and E) had a consistent offset in the $\triangle$pH$^{mCP\text{-}FET}$ where mCP pH values were greater than 0.05 pH units higher than the ISFET pH. There was a significant difference between experienced and novice groups in pier deployments and flowthrough systems (Mann–Whitney Rank Sum Test, Fig. 4(A) and (B)). There was no significant difference between ISFET sensors in the SeaFET configuration (either the commercially available version from Satlantic or the prototype versions) and Honeywell configuration (comparing experienced deployments only, Mann–Whitney Rank Sum Test), nor for deployment environment: pier, flowthrough system, or buoy (comparing experienced deployments only, Mann–Whitney Rank Sum Test, Fig. 4(C)).

The mean difference between the pH value calculated from DIC and TA and the ISFET sensor pH ($\triangle$pH$^{calc\text{-}FET}$) across all
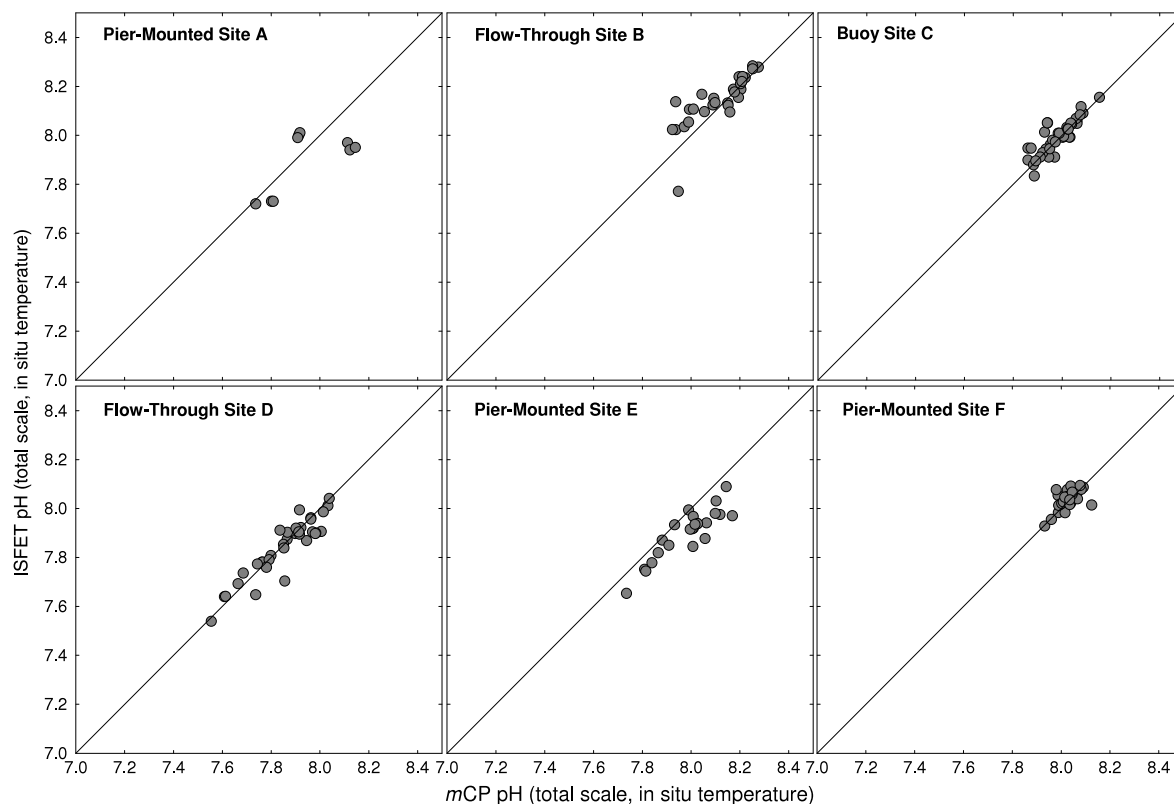
Fig. 3. Difference in pH between ISFET sensor and pH measured in the laboratory using the *m*-cresol purple (*m*CP method) for each site and across sites.

Table 4
Site by site comparison of sensor performance relative to discrete standard.

Station	Mean $\Delta \pm 2\sigma$ *m*CP pH−calculated pH (DIC and TA) (ΔpH$^{mCP\text{-}calc}$)	Mean $\Delta \pm 2\sigma$ *m*CP pH−ISFET pH (ΔpH$^{mCP\text{-}FET}$)	Mean $\Delta \pm 2\sigma$ calculated pH−ISFET pH (ΔpH$^{Calc\text{-}FET}$)
Pier-mounted site A	−0.001 ± 0.055	0.048 ± 0.230	0.076 ± 0.215
Flowthrough site B	−0.013 ± 0.066	−0.030 ± 0.138	−0.019 ± 0.149
Buoy site C	−0.009 ± 0.099	−0.012 ± 0.078	0.002 ± 0.140
Flowthrough site D	−0.028 ± 0.090	0.011 ± 0.101	−0.039 ± 0.146
Pier-mounted site E	−0.012 ± 0.057	0.083 ± 0.104	0.089 ± 0.099
Pier-mounted site F	−0.020 ± 0.067	−0.020 ± 0.063	−0.004 ± 0.058

sites was 0.021 (Table 3). Calculated pH and spectrophotometric pH demonstrated similar site to site variation in the difference between the laboratory pH and the ISFET pH (Table 4), with the notable exception of Site C, where the calculated pH had nearly double the range of variability compared to the spectrophotometric pH. This is likely attributable to the fact that the mooring at Site C is located at the mouth of a slough and the high organic carbon loading and/or contribution of non-carbonate anions to total alkalinity from the slough could interfere with calculation of pH (Hunt et al., 2011; Wootton and Pfister, 2012).

4. Discussion

Calibrated ISFET sensors have been shown to operate with an accuracy of 0.01 pH units or better on the total proton scale and have demonstrated stability over weeks to months of ±0.005 pH units when deployed by experienced specialists (Martz et al., 2010; Johnson et al., 2016). However, we observed considerable instrument/operator-specific variability in agreement between the bottle measurements of pH and ISFET measures, particularly for first-time operators, with experienced operators having significantly greater accuracy and greater precision in sensor measurements compared to novice operators (Fig. 4(A) and (B)).

Up to half the observed difference between sensors and discrete samples can be attributable to uncertainty associated with the discrete, reference sample measurement, as evidenced by the average 0.011 pH unit difference between replicate pH samples collected by the same operator and the average −0.015 pH unit difference between the spectrophotometric and calculated measures. Previous research suggests one should be able to estimate pH on a discrete sample spectrophotometrically with an associated uncertainty of ±0.005 (Carter et al., 2013) and calculate pH from DIC and TA with an associated uncertainty of ±0.02 (Dickson and Riley, 1978; Dickson et al., 2003); however, most coastal field studies report much higher uncertainty [0.01–0.05 pH units Wootton and Pfister, 2012; Hammer et al., 2014]. Some additional error could also be associated with where we collected the discrete sample, as the coastal ambient environment is characterized by considerable small-scale spatial and temporal variability (Frieder et al., 2012). Site D, for example, used a flowthrough system in which the validation sample was collected downstream of the sensor measurement and had a ±2σ standard deviation between laboratory standard and sensor pH of ±0.1 pH units (Table 4). This site also had one of the highest rates of ambient change in this study (an average of 0.084 pH units per hour, Table 5). In this case, the rate of change in pH could impart an average difference of 0.01 in pH over the five minutes it could take to fill two discrete sample bottles for replicate
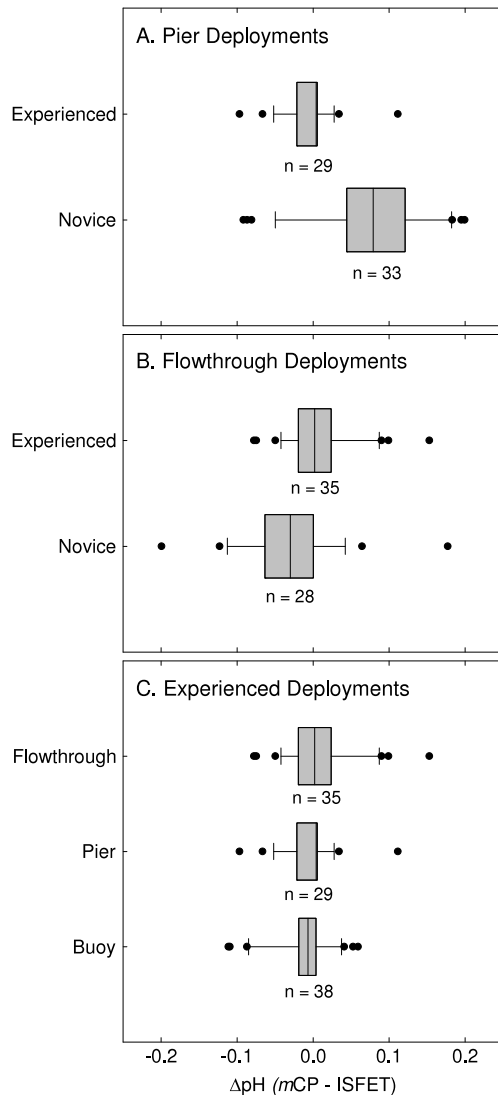
Fig. 4. Experienced users had significantly better agreement between ISFET sensor measurements and bottle sample measurements (Mann–Whitney Rank Sum Test) on pier deployments (A, $P < 0.001$) and in flowthrough systems (B, $P = 0.004$). There were no significant differences (Mann–Whitney Rank Sum Test) between experienced operators on the pier, buoy, or flowthrough system deployments (C).
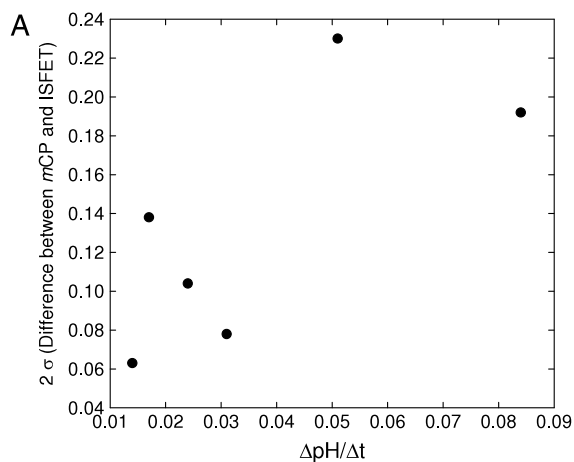
analysis, which were collected in sequence from the flowthrough system, and could potentially impart a greater difference during periods of more rapid ambient pH change. In this study, the $\pm 2\sigma$ standard deviation between laboratory measurement and sensor pH increases as the overall range of observed pH values increases, which may suggest that the spatial and temporal variability of pH may be a component of the difference between discrete and sensor values (Fig. 5). Thus, an offset in time and/or space would be expected to impart a difference between bottle and sensed pH in nearshore areas, particularly those areas with large natural ranges in pH.

The remainder of the observed differences between sensors and discrete samples appears to be attributable to operator error in use of the ISFET sensors, most of which was associated with calibration and biofouling/sensor malfunction. Best practices suggest a careful laboratory-based calibration point based on a discrete sample(s), following conditioning of the ISFET (Bresnahan et al., 2014). An extended conditioning period of the sensor to ambient water was only apparent at one site (site A), resulting in a large amount of early deployment data that failed quality control screening (Table 2). The sites that conducted a post-conditioning calibration performed better, though problems with calibration may contribute to a consistent bias in the difference between the discrete and sensor values (i.e., sites where the average difference was significantly different from zero). Novice sites had average differences between bottle and sensor pH greater than ± 0.03 pH units, which may indicate some level of error that may be resolved through improved calibration. Very little additional uncertainty seems to be added by the sensors themselves, evidenced by the fact that the most experienced operators (Sites C and F) had average $\Delta pH^{mCP-ISFET}$ and $\Delta pH^{Calc-ISFET}$ that are indistinguishable from the average difference between replicate pH samples and the average $\Delta pH^{mCP-Calc}$.

Sensor drift towards the end of the deployments were apparent in all of the datasets to varying degrees, resulting in data loss during quality control screening (Table 2, Supplemental Figure 1, Appendix A). Bresnahan et al. (2014) have suggested co-deployment of another, independent pH sensor or other parameter sensor(s) that would be expected to co-vary with pH to monitor for sensor drift when confidence in data quality is critical.

While opportunities remain for improving the performance of the ISFET sensors when deployed by less experienced operators, the uncertainty associated with their deployment and validation was several-fold less than the natural temporal variability observed in this study. The 'natural' variability at each site, defined as the range of pH units encompassing 90% of all observed pH values,
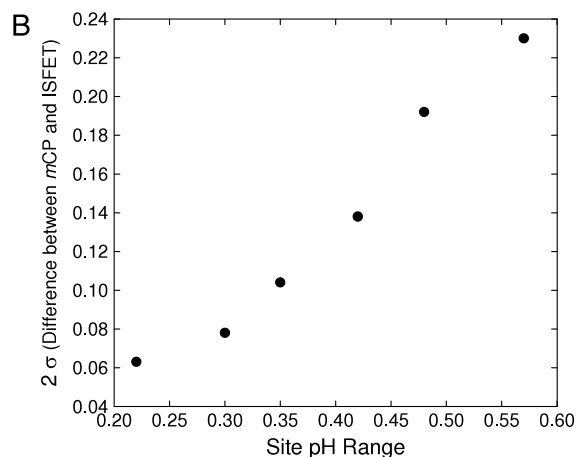

Fig. 5. Two sigma standard deviation in the difference between spectrophotometric pH (*m*CP) and ISFET sensor pH increases with both the rate of change in pH at each site (A) as well as the pH range at each site (B).
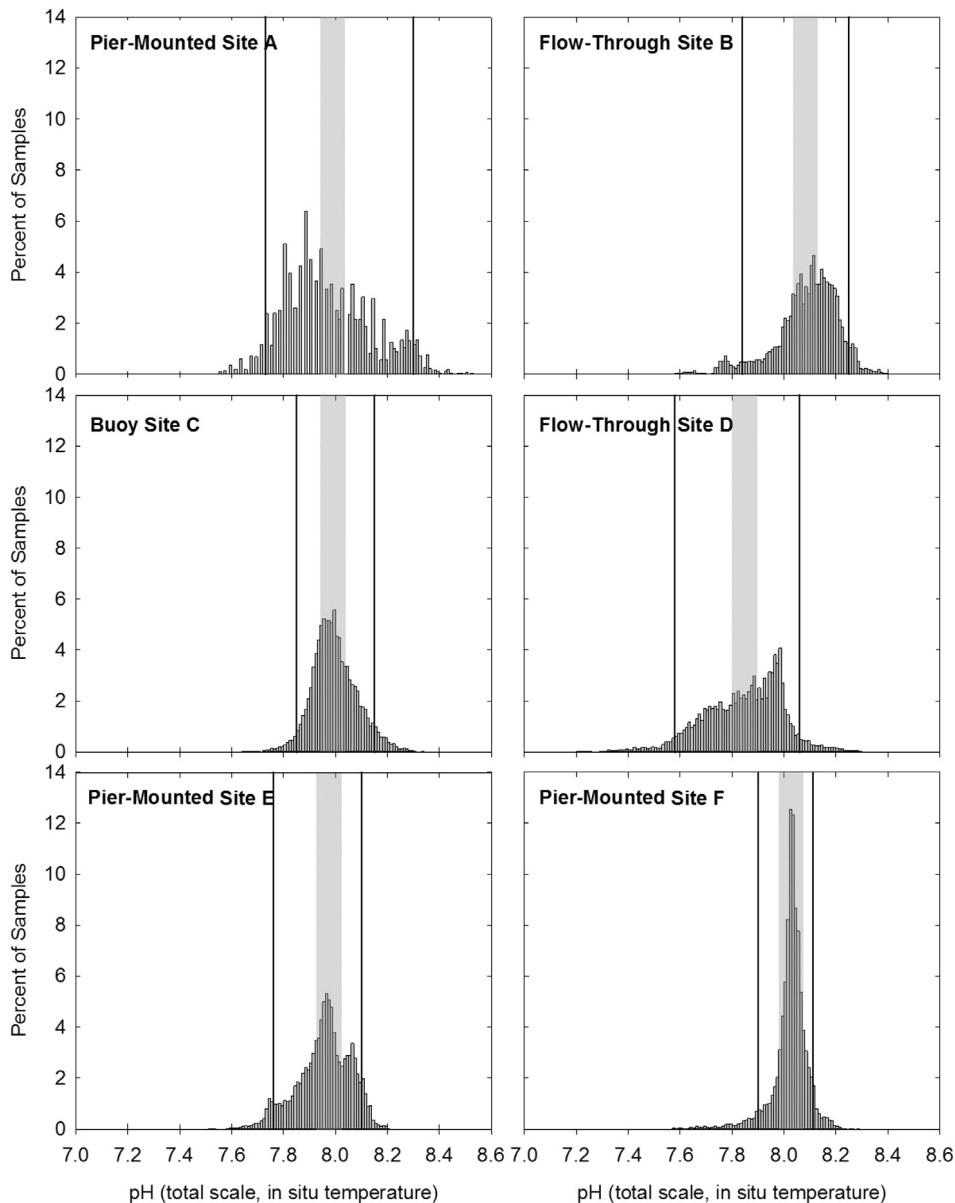
Fig. 6. Natural ranges of pH at each of the 6 sites. Solid black lines represent the 5th and 95th percentile of observed pH at each site. Shaded grey square represents an uncertainty of ISFET sensor measurements of ±0.05 around the mean pH at each site.

ranged from 0.57 pH units to 0.22 pH units, with an average of 0.39 pH units (Table 5, Fig. 6). Given the site with the best $\Delta pH^{mCP\text{-}FET}$ is in the range of 0.01–0.02 pH units, the ISFET sensors would be able to discern trends and patterns in environments with natural ranges greater than 0.1 pH units. However, in a network context, where data may be present from multiple locations, uncertainty in spatial comparisons could be higher, as much as 0.2 pH units, depending on the experience level of the participating operators.

5. Conclusions

ISFET sensors can provide information on high frequency pH variability within defined error limits in nearshore marine deployments given appropriate experience with sensors and use of best practices to ensure data quality. Nevertheless, operators should be cautioned that operator error appears to be a defining factor in generating usable data with an ISFET sensor. Operator errors in collecting and analyzing discrete samples, as well as improper calibration and deployment of the ISFET, are factors

that can be mitigated through training and use of best practices (Bresnahan et al., 2014; Rivest et al., 2016). This study suggests that differences between calibrated sensor pH values and values obtained from discrete, check samples can be expected to be as small as 0.02 pH units, and perhaps less. Given this, most sites would be expected to recover data with uncertainties that reflect those of the highest-performing sites in this study. Best practices to identify and reduce sensor measurement error related biofouling will improve data recovery. Our experience supports the (Bresnahan et al., 2014) recommendation that co-deployment of at least one other independent sensor would provide confirmation that the sensors are not drifting and greatly improve confidence in data quality.

Table 5
Range of pH conditions encountered at the six test sites.

Station	Max pH	Min pH	Average $\Delta pH/\Delta t$ (pH units hr^{-1})	pH range between the 5th and 95th percentile
Pier-mounted site A	8.52	7.55	0.051	0.57
Flowthrough site B	8.40	7.58	0.017	0.42
Buoy site C	8.37	7.43	0.031	0.30
Flowthrough site D	8.33	7.10	0.084	0.48
Pier-mounted site E	8.21	7.43	0.024	0.35
Pier-mounted site F	8.30	7.56	0.014	0.22

Appendix A. Supplementary data

Supplementary material related to this article can be found online at http://dx.doi.org/10.1016/j.rsma.2017.02.008.

References

Boehm, A.B., Jacobson, M.Z., O'Donnell, M.J., Sutula, M., Wakefield, W.W., Weisberg, S.B., Whiteman, E., 2015. Ocean acidification science needs for natural resource managers of the North American West Coast. Oceanography 28.

Borges, A.V., Gypens, N., 2010. Carbonate chemistry in the coastal zone responds more strongly to eutrophication than to ocean acidification. Limnol. Oceanogr. 55, 346–353.

Bresnahan, P.J., Martz, T.R., Takeshita, Y., Johnson, K.S., LaShomb, M., 2014. Best practices for autonomous measurement of seawater pH with the Honeywell DuraFET. Methods Oceanogr. 9, 44–60.

Carter, B.R., Radich, J.A., Doyle, H.L., Dickson, A.G., 2013. An automated system for spectrophotometric seawater pH measurements. Limnol. Oceanogr.-Methods 11, 16–27.

Dickson, A.G., 2001. Reference materials for oceanic measurements. Oceanography 14, 21–22.

Dickson, A.G., Afghan, J.D., Anderson, G.C., 2003. Reference materials for oceanic CO$_2$ analysis: A method for the certification of total alkalinity. Mar. Chem. 80, 185–197.

Dickson, A., Riley, J., 1978. The effect of analytical error on the evaluation of the components of the aquatic carbon-dioxide system. Mar. Chem. 6, 77–85.

Dickson, A.G., Sabine, C.L., Christian, J.R. (Eds.), 2007. Guide to Best Practices for Ocean CO$_2$ Measurements.

Dickson, A.G., Wesolowski, D.J., Palmer, D.A., Mesmer, R.E., 1990. Dissociation constant of bisulfate ion in aqueous sodium chloride solutions to 250 degree C. J. Phys. Chem. 94, 7978–7985.

Doney, S.C., Fabry, V.J., Feely, R.A., Kleypas, J.A., 2009. Ocean acidification: The other CO$_2$ problem. Pages 169–192 Annual Review of Marine Science. Annual Reviews, Palo Alto.

Fabry, V.J., Seibel, B.A., Feely, R.A., Orr, J.C., 2008. Impacts of ocean acidification on marine Fauna and ecosystem processes. ICES J. Mar. Sci.: J. Conseil 65, 414–432.

Frieder, C.A., Nam, S.H., Martz, T.R., Levin, L.A., 2012. High temporal and spatial variability of dissolved oxygen and pH in a nearshore California kelp forest. Biogeosciences 9, 3917–3930.

Hammer, K., Schneider, B., Kuliński, K., Schulz-Bull, D.E., 2014. Precision and accuracy of spectrophotometric pH measurements at environmental conditions in the Baltic Sea. Estuar. Coast. Shelf Sci. 146, 24–32.

Hofmann, G.E., Smith, J.E., Johnson, K.S., Send, U., Levin, L.A., Micheli, F., Paytan, A., Price, N.N., Peterson, B., Takeshita, Y., 2011. High-frequency dynamics of ocean pH: A multi-ecosystem comparison. PLoS One 6, e28983.

Hoppe, C.J.M., Langer, G., Rokitta, S.D., Wolf-Gladrow, D.A., Rost, B., 2012. Implications of observed inconsistencies in carbonate chemistry measurements for ocean acidification studies. Biogeosciences 9, 2401–2405.

Howarth, R., Chan, F., Conley, D.J., Garnier, J., Doney, S.C., Marino, R., Billen, G., 2011. Coupled biogeochemical cycles: Eutrophication and hypoxia in temperate estuaries and coastal marine ecosystems. Front. Ecol. Environ. 9, 18–26.

Hunt, C., Salisbury, J., Vandemark, D., 2011. Contribution of non-carbonate anions to total alkalinity and overestimation of pCO$_2$ in New England and New Brunswick rivers. Biogeosciences 8, 3069–3076.

Johnson, K.S., Jannasch, H.W., Coletti, L.J., Elrod, V.A., Martz, T.R., Takeshita, Y., Carlson, R.J., Connery, J.G., 2016. Deep-sea DuraFET: A pressure tolerant pH sensor designed for global sensor networks. Anal. Chem. 88, 3249–3256.

Kroeker, K.J., Micheli, F., Gambi, M.C., Martz, T.R., 2011. Divergent ecosystem responses within a benthic marine community to ocean acidification. Proc. Natl. Acad. Sci. 108, 14515–14520.

Lee, K., Kim, T.-W., Byrne, R.H., Millero, F.J., Feely, R.A., Liu, Y.-M., 2010. The universal ratio of boron to chlorinity for the North Pacific and North Atlantic oceans. Geochim. Cosmochim. Acta 74, 1801–1811.

Liu, X., Patsavas, M.C., Byrne, R.H., 2011. Purification and charaterization of meta-cresol purple for spectrophotometric seawater pH measurements. Environ. Sci. Technol. 45, 4862–4868.

Lueker, T.J., Dickson, A.G., Keeling, C.D., 2000. Ocean pCO(2) calculated from dissolved inorganic carbon, alkalinity, and equations for k-1 and k-2: Validation based on laboratory measurements of CO$_2$ in gas and seawater at equilibrium. Mar. Chem. 70, 105–119.

Martz, T.R., Connery, J.G., Johnson, K.S., 2010. Testing the Honeywell DuraFET$^®$ for seawater pH applications. Limnol. Oceanogr. Methods 8, 172–184.

McLaughlin, K., Weisberg, S.B., Dickson, A.G., Hofmann, G.E., Newton, J.A., Aseltine-Neilson, D., Barton, A., Cudd, S., Feely, R.A., Jefferds, I.W., Jewett, E.B., King, T., Langdon, C., McAfee, S., Pleschner-Steele, D., Steele, B., 2015. Core principles for a nearshore marine acidification monitoring network: Linking chemistry, physics and ecological effects. Oceanography 28, 160–169.

Newton, J.A., Feely, R.A., Jewett, E.B., Williamson, J., Mathis, J., 2014. Global Ocean Acidification Observing Network: Requirements and governance plan. http://www.goa-on.org/docs/GOA-ON_plan_print.pdf.

Rivest, E.B., O'Brien, M., Kapsenberg, L., Gotschalk, C.C., Blanchette, C.A., Hoshijima, U., Hofmann, G.E., 2016. Beyond the benchtop and the benthos: Dataset management planning and design for time series of ocean carbonate chemistry associated with DuraFET$^®$-based pH sensors. Ecol. Inform..

Robbins, L.L., Hansen, M.E., Kleypas, J.A., Meylan, S.C., 2010. CO2calc– a user friendly seawater carbon calculator for Windows, Mac OSX, and iOS (iPhone): US Geological Survey open-file report 2010–1280.

Wootton, J.T., Pfister, C.A., 2012. Carbon system measurements and potential climatic drivers at a site of rapidly declining ocean pH. PLoS One 7, e53396.

Yu, P.C., Matson, P.G., Martz, T.R., Hofmann, G.E., 2011. The ocean acidification seascape and its relationship to the performance of calcifying marine invertebrates: Laboratory experiments on the development of urchin larvae framed by environmentally-relevant pCO$_2$/pH. J. Exp. Mar. Biol. Ecol. 400, 288–295.